THE JOURNAL OF PHYSICAL CHEMISTRY B LETTERS

2007, *111,* 11622−11625
Published on Web 09/14/2007

Nanoscale Energy Deposition by X-ray Absorbing Nanostructures

Joshua D. Carter, Neal N. Cheng, Yongquan Qu, George D. Suarez, and Ting Guo*

Department of Chemistry, University of California, One Shields Avenue, Davis, California 95616

Received: July 5, 2007; In Final Form: August 23, 2007

Here we wish to demonstrate a unique property of nanomaterials: energy deposition with nanometer precision from low-energy electrons released from these nanostructures interacting with hard X-ray radiation in aqueous solution. Three effects combine to cause this phenomenon: (1) localized absorption of X-rays by nanostructures, (2) effective release of low-energy electrons from small nanostructures, and (3) efficient deposition of energy in water in the form of radicals and electrons. This combination creates localized X-ray absorption and localized energy deposition of nanometer precision. We confirmed the theoretically predicted nanoscale energy deposition distribution by measuring hydroxyl radical-induced DNA strand breaks, and observed enhanced damage to a 5600-bp DNA molecule from approximately 10 chemically conjugated small gold nanoparticles under X-ray radiation. These results provide a general guidance to applications of this new concept in many fields including radiation chemistry, radiology, radiation oncology, biochemistry, biology, and nanotechnology.

Nanomaterials possess many unique properties such as the quantum size effect, large surface-to-volume ratios, multiple surface sites available for chemical binding, and intense plasmon resonance-induced absorption bands created by the unique geometry of these nanomaterials. All of these properties have led to numerous scientific and technological breakthroughs in the last two decades.[1−6] X-ray radiation interacts with matter, including nanomaterials, through scattering, excitation, and/or ionization of the electrons in the atoms. An early work showed that there was ∼30−50% increased radiation damage to tumors loaded with X-ray-absorbing metal microspheres at 1% by weight.[7] The result suggested that the added metals may absorb more X-rays and release more electrons into the solution, which in turn interact with water molecules to produce radicals.[8,9] Although most studies suggest that DNA is damaged indirectly by hydroxyl radicals,[10] electrons can also cause damage to DNA directly, as illustrated in a recent study in which low-energy electrons emitted from metal films were found to cause DNA strand breaks directly.[11] Another example of using electrons released from chemicals to damage DNA is Auger therapy or photon activated therapy (PAT) using atomic species such as iodine complexes embedded in DNA to increase the absorption of radiation and hence the yield of electrons and reactive species such as radicals around the target DNA.[12−17] On the basis of the assumption that nanomaterials can absorb more external radiation within a small volume, nanomaterials have been used to enhance X-ray damage to DNA or to help cure cancer-bearing mice.[18,19] However, even though it is straightforward to understand that nanoparticles can absorb X-rays more locally (e.g., a nanoparticle containing ∼1000 atoms occupies only a 3-nm-diameter sphere, whereas 1000 separate atomic species spread into a much larger volume of over 10^6 nm^3 at 1 mM concentration), and it is possible to deliver a 3-nm nanoparticle but never 1000 atoms to a location such as a specific nucleotide in a DNA molecule, it is unclear whether the geometric precision of the energy deposition of released electrons upon absorption of X-ray radiation by these nanoparticles is of nanoscale or macroscopic nature. The impact of such an understanding can be significant. For example, if the released electrons and radicals are indeed localized within nanometers of the added nanomaterials, then it is worthwhile to develop targeted delivery of nanoparticles to specific sites to create precisely targeted damage to biological samples such as DNA molecules. Otherwise, it is unnecessary to even attempt to deliver nanostructures into the cell if the electrons or radicals are deposited over a large volume.

To elucidate the mechanisms of energy deposition, a Monte Carlo method was developed to investigate the generation and transport of electrons in nanomaterials dissolved in water.[34] We chose to model small gold nanoparticles that were available to us experimentally. Figure 1 shows a schematic diagram of these nanostructures (3-nm gold nanoparticles) and a biological target of DNA [∼500 nm long and 1.5 nm diameter supercoiled DNA (scDNA)]. In the simulation, X-rays from a 100-kVp tungsten source interact directly with water and gold to produce Auger electrons, Compton electrons, secondary electrons, and photoelectrons. All of these electrons are capable of interacting with water to produce radicals, or with the nanostructures to produce more electrons. For X-rays of much higher energy (>1 MeV), Compton scattering of X-rays may occur in nanostructures and pair production may occur in both water and gold. These processes are not considered here because the X-ray energy is less than 100 keV. The simulated results show that a majority of the electrons emitted from the 3- to 4-nm gold nanoparticles escape the nanoparticles, and more importantly many low-energy electrons (<100 eV) are created during the escaping process. The number of these low-energy electrons is reduced significantly when the size is greater than 6 nm. The penetration distance of the escaped electrons in water ranges from a few

* Corresponding author. E-mail: tguo@ucdavis.edu; (530) 754-5283 (tel); (530) 752-8995 (fax).

10.1021/jp075253u CCC: $37.00

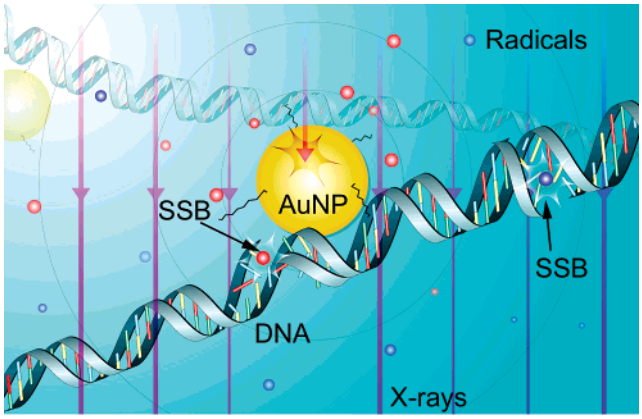

Figure 1. Schematic diagram of the results of the Monte Carlo simulation. Two DNA segments (not a scDNA) are shown. Also shown are the radicals (blue spheres, distributed evenly) generated from electrons produced in water, as well as radicals (red spheres, concentrated near the nanoparticle) from Auger electrons, secondary and photoelectrons electrons originated from the gold nanoparticle (AuNP). When the radicals are within ~0.5 nm of the scDNA, a single-strand break (SSB) occurs with ~25% efficiency. The trajectories of electrons are not shown, and only the relative average density of radicals generated from these electrons is displayed. The diameter of the AuNP shown here is approximately 3 nm.

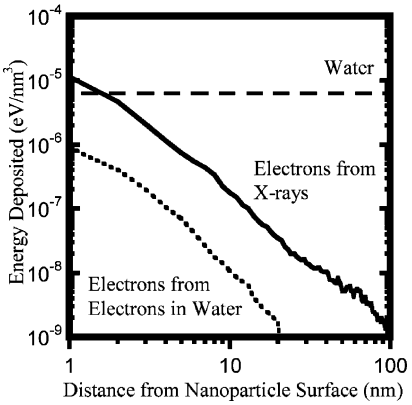

Figure 2. Results of the Monte Carlo simulation of transport of average energy deposition of electrons released from a 3-nm gold nanoparticle in water. A large portion of the low-energy Auger and secondary electrons were stopped within a 5-nm-radius sphere after escaping the nanostructures, whereas photoelectrons from these nanomaterials travel much farther. Energy deposition of gold nanoparticles interacting with X-rays (solid line) and with Compton electrons and photoelectrons from water (dotted line), as well as the average energy deposition obtained from X-ray interaction with water (dashed line), are shown. X-ray flux is fixed at 3.21×10^{10} photons/cm^2/s for 60 s in these calculations. This dose is equivalent to 1 Gy of absorbed radiation in water.

nanometers for low-energy electrons to many micrometers for high-energy electrons (>10 keV). The main channel of electron energy loss is through radical generation. The low-energy electrons are typically known as high linear-energy-transfer (LET) particles, meaning that they can lose energy quickly. In our simulation, although all of the electrons travel in distinct trajectories (spurs, bulbs, and short tracks),[20] we used an average energy deposition to characterize the energy deposition processes. The density of average (over space and nanoparticles) energy deposition (eV/nm^3) per 1 Gy of absorbed radiation water as a function of distance for each 3-nm nanoparticle is shown in Figure 2 (solid line). As shown, the density decreases quickly as the distance increases, lowering by nearly 4 orders of magnitude from 1 to 100 nm. This profile can be converted directly to the density of radicals in the so-called prechemical phase,[21] and it resembles closely the spatial profile of the radicals even with diffusion taken into consideration, as long as the diffusion distance is much shorter than 100 nm, as in the intracellular environment.[22] The radical distribution (red spheres) created from electrons emitted from gold nanoparticles is shown schematically in Figure 1, which also illustrates the difference between these radicals and those generated from electrons produced in water (blue spheres). The former concentrate near the nanoparticles, whereas the latter are distributed evenly in water. Because high-energy electrons generated elsewhere in water can still travel a long distance (many micrometers or greater) to reach a target even in the cell environment, their role of generating secondary electrons after collisions with nanostructures has to be considered. The energy deposition via electron−nanoparticle (dotted line) interactions and that from water (dashed line) are shown in Figure 2. It shows that for X-rays from a 100 keV source the X-ray−nanoparticle interactions dominate the process.

Although it is difficult to probe directly the nanoscale spatial profile of energy deposition created by nanostructures in aqueous solution, it is possible to use biological samples such as DNA molecules in a controlled environment to indirectly detect this energy distribution. Most damage incurred to DNA in dilute aqueous solution exposed to ionizing radiation is caused by reactions between DNA and hydroxyl radicals that are generated from the interaction of Compton electrons and photoelectrons with water.[8] When gold nanoparticles are present, the electrons released from these nanoparticles create more radicals. Therefore, the precision of DNA strand break measurements rely on the profile of electron energy deposition and the diffusion distance of radicals in water. For electrons generated from water, the profile of deposition is uniform (Figure 2), and therefore DNA damage is the same everywhere. For nanoparticles, the profile has a maximum near the nanoparticles (solid line, Figure 2). However, because radicals can diffuse over a long distance in pure water, the precision of using DNA strand breaks to characterize the electron energy deposition profile is low. In addition, radicals from a large body of water contribute to the damage of DNA in pure water, making it nearly impossible to detect a small amount of DNA damage caused by a small amount of added nanomaterials. Fortunately, it is possible to add radical scavengers such as a Tris base in water to reduce the diffusion distance of hydroxyl radicals, all the way down to a few nanometers or less.[23,24] In such a case, the effective volume of water contributing to the background radical generation is reduced greatly, making it easy to detect the DNA damage caused by added nanomaterials. More critically, the nanometer resolution afforded by the scavengers also makes it possible to characterize the profile of electron energy deposition of the gold nanoparticles.

We used gold nanoparticles conjugated to scDNA via an ethidium-based intercalating ligand to experimentally probe the energy deposition distribution from small nanoparticles. In this experiment, 3-nm (2.8 ± 1.0 nm) gold nanoparticles covered with a mixture of ethidium thiol ligands (<10 ligands per nanoparticle) and charge-neutral surfactants were prepared.[35] The charge-neutral ligands were used to avoid DNA aggregation and possible nonlinear damage,[25] and such a small amount of ethidium in the samples (<150 nM) did not yield any detectable change to scDNA. The ratio of nanoparticles to scDNA was ~10. Figure 3A shows a transmission electron microscope (TEM) image of nanoparticle-conjugated scDNA in which all of the nanoparticles were shown to conjugate to scDNA. The distance between the nanoparticles and DNA was less than 2 nm, separated only by the surfactants (~1.5 nm long) on the

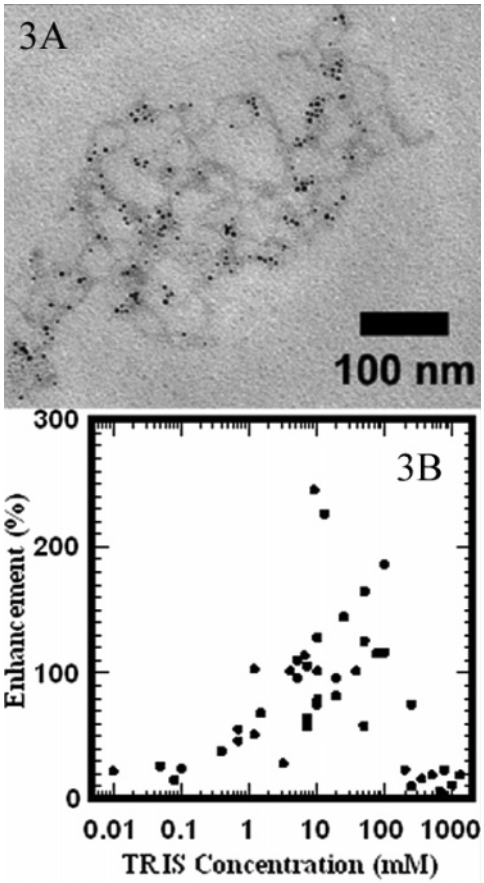

Figure 3. (A) Transmission electron microscope image of scDNA with gold nanoparticles conjugated to them. The scDNA were stained to increase contrast. Each scDNA has ~10 nanoparticles attached to it. All nanoparticles are conjugated to the scDNA. (B) Radiation enhancement of damage to scDNA conjugated to gold nanoparticles. The enhancement was defined as the additional single-strand breaks (SSBs) to scDNA conjugated gold nanoparticles divided by that without gold nanoparticles under otherwise identical experimental conditions.

surface of the gold nanoparticles. As mentioned above, Tris base was added to control the diffusion distance of hydroxyl radicals in water.[26] Figure 3B shows the results of DNA damage as a function of Tris concentration. At low concentrations, the enhanced damage to scDNA by gold nanoparticles compared to that without the nanoparticles was nearly zero because radicals generated from a large volume of background water diffused to and react with scDNA. As the scavenger concentration increased, the enhancement increased as well (because the diffusion distance of radicals and the effective water volume contributing to the DNA strand breaks became smaller).[26] On the basis of the enhancement peaked near 100 mM, only energy deposited within ~5 nm of the scDNA was effective in generating radicals that may diffuse to scDNA to cause strand breaks. When the Tris concentration was too high, it scavenged even the radicals generated locally from nanoparticles near the target, thus reducing the enhancement. Because of the small amount of gold nanoparticles used here, the damage by high-energy photoelectrons emitted from these nanoparticles was negligible compared to that of water. The high Tris concentration results also suggested that contribution from direct electron ionization/attachment by electrons released from these approximately 10 nanoparticles per scDNA was negligible. Ethidium ligands alone with scDNA under radiation did not yield any enhancement. No enhancement was observed for nonconjugated nanoparticles (same nanoparticles as described above but without the ethidium intercalating ligand) at up to a few micromolar concentration. These results clearly demonstrated that the enhancement from conjugated nanoparticles is of nanoscale nature.

The single-strand breaks (SSBs) generated from the hydroxyl radicals and the enhancement may be estimated based on the amounts of radicals generated from the effective volume of water and gold nanoparticles, respectively. Using the SSB yield of DNA in 0.5 M Tris base predicted in the literature, which corresponds to $\sim 2.8 \times 10^{-7}$ $Gy^{-1}bp^{-1}$,[21] and assuming that no more than one SSB per scDNA occurred in our experimental measurements because we limited the damage of scDNA by X-ray radiation to ~20%, the damage of 5600 bp scDNA from radicals generated from water is calculated to be ~3%. Factoring the difference in Tris base (100 mM in our work vs 0.5 M mentioned above), the estimated damage is relatively close to what we observed experimentally. On the basis of the diffusion of radicals in 100 mM Tris base solution, the diffusion distance of radicals is estimated to be 5.0 nm (see the Supporting Information). Using this value and the values given in Figure 2, we estimate the damage due to water alone should be ~35% for 100 Gy of radiation absorbed, which is twice the experimental value (20%). This leads us to believe that scDNA molecules are at least doubly coiled in water. For exactly 10 3-nm-diameter nanoparticles in a 250-nm-long cylinder (due to the fact that scDNA molecules are coiled) that contains a scDNA molecule, the average energy deposition by X-ray absorbing gold nanoparticles is 20% of that of water within the 5.0-nm-radius cylinder. As explained before, the ratio of the amounts of radicals generated from gold nanoparticles and water should be close to that of the energy deposited from these two materials when the diffusion distance of the radicals is small. This means that the average enhancement of DNA damage caused by hydroxyl radicals should also be ~20%, which is lower than what we observed experimentally (150% at 100 mM Tris). This difference may be caused by several factors, including that the real size and number of nanoparticles may be different from the ones used in the calculation, that scDNA molecules are temporarily cross-linked in solution during radiation, that radicals generated from nanoparticles are more reactive because they are closer to scDNA, and that many nanoparticles may be located at the interactions of several double-stranded DNA segments. Future effort will be directed to fully account for the experimentally observed enhancement.

The results presented here clearly show that a combined high efficiency of X-ray absorption by nanostructures and localized energy deposition of electrons and radicals near these nanostructures can create precisely controlled energy deposition and hence a new nanoscale phenomenon. If these nanostructures can be delivered to specific sites, whether it is in vivo or in vitro, then this technique can be used to create highly localized electron and radical deposition, which may be useful for studying biochemistry, radiation chemistry, biophysics, radiation oncology, radiology, nanotechnology, genomics, and nanomedicine. In contrast, if these nanomaterials are not conjugated to the target, then a much greater amount of them (several orders of magnitude more) has to be used to achieve enhanced radiation damage. Further enhancement may be achieved with optimization of the composition, size, and shape of these nanostructures. In combination with recently developed targeted drug delivery, a specific application is cancer treatment with these nanostructures.[27−29]

Acknowledgment. We thank Professor C. F. Meares for insightful discussion and experimental assistance. We thank Ms. T. Huynh, Dr. F. Shan, and Ms. Z.G. Smith for their experimental assistance. This work is supported by a University of

California and Lawrence Livermore National Lab Collaborative Grant and partially supported by the National Science Foundation (CHE-0135132).

Supporting Information Available: Energy deposition through the interaction of water with individual electrons released from water and gold nanoparticles as a result of X-ray absorption and scattering is simulated using the Monte Carlo method. The simulation keeps track of each of these electrons and any secondary electrons generated from these electrons. Energies deposited from X-rays interacting with water and gold nanoparticles are calculated separately, and the enhancement of X-ray damage to scDNA is calculated using the ratio of these two energies integrated over the specified space. The effect of scavengers is estimated using the diffusion of radicals and the rate equations for the reactions between radicals and scavengers and among radicals themselves. The preparation of the ligands and nanoparticles used in this work and the procedures of attaching the nanoparticle to scDNA for X-ray radiation testing are described. Results of the control experiments demonstrating that much larger amounts of unconjugated nanoparticles led to no enhancement in radiation damage are also presented. This material is available free of charge via the Internet at http://pubs.acs.org.

References and Notes

(1) Cullis, A. G.; Canham, L. T. *Nature* **1991**, *353*, 335.
(2) Evans, D. A.; Alonso, M.; Cimino, R.; Horn, K. *Phys. Rev. Lett.* **1993**, *70*, 3483.
(3) Benfield, R. E. *J. Chem. Soc., Faraday Trans.* **1992**, *88*, 1107.
(4) Alivisatos, A. P. *Science* **1996**, *271*, 933.
(5) Xiong, Y.; Mayers, B.; Xia, Y. *Chem. Commun.* **2005**, 5013.
(6) West, J. L.; Halas, N. J. *Annu. Rev. Biomed. Eng.* **2003**, *5*, 285.
(7) Herold, D.; Das, I.; Stobbe, C.; Iyer, R.; Chapman, J. *Int. J. Radiat. Biol.* **2000**, *76*, 1357.
(8) von Sonntag, C. *The Chemical Basis for Radiation Biology*; Taylor and Francis: London, 1987.
(9) Turner, J. E.; Magee, J. L.; Wright, H. A.; Chatterjee, A.; Hamm, R. N.; Ritchie, R. H. *Radiat. Res.* **1983**, *96*, 437.
(10) Chatterjee, A.; Magee, J. L. *Radiat. Prot. Dosim.* **1985**, *13*, 137.
(11) Boudaiffa, B.; Cloutier, P.; Hunting, D.; Huels, M. A.; Sanche, L. *Science* **2000**, *287*, 1658.
(12) Fairchild, R. G.; Bond, V. P. *Strahlentherapie* **1984**, *160*, 758.
(13) Laster, B. H.; Thomlinson, W. C.; Fairchild, R. G. *Radiat. Res.* **1993**, *133*, 219.
(14) Hofer, K. G. *Acta Oncol.* **2000**, *39*, 651.
(15) Kassis, A. I. *J. Nucl. Med.* **2003**, *44*, 1479.
(16) Karnas, S. J.; Moiseenko, V. V.; Yu, E.; Truong, P.; Battista, J. J. *Radiat. Environ. Biophys.* **2001**, *40*, 199.
(17) Kobayashi, K.; Usami, N.; Sasaki, I.; Frohlich, H.; Le Sech, C. *Nucl. Instr. Methods Phys. Res., Sect. B* **2003**, *199*, 348.
(18) Foley, E.; Carter, J.; Shan, F.; Guo, T. *Chem. Commun.* **2005**, 3192.
(19) Hainfeld, J. F.; Slatkin, D. N.; Smilowitz, H. M. *Phys. Med. Biol.* **2004**, *49*, N309.
(20) Farhataziz; Rodgers, M. A. J. *Radiation Chemistry: Principles and Applications*; VCH Publishers, Inc.: New York, 1987.
(21) Moiseenko, V. V.; Hamm, R. N.; Waker, A. J.; Prestwich, W. V. *Int. J. Radiat. Biol.* **1998**, *74*, 533.
(22) Roots, R.; Okada, S. *Radiat. Res.* **1975**, *64*, 306.
(23) Krisch, R. E.; Flick, M. B.; Trumbore, C. N. *Radiat. Res.* **1991**, *126*, 251.
(24) Stanton, J.; Taucherscholz, G.; Schneider, M.; Heilmann, J.; Kraft, G. *Radiat. Environ. Biophys.* **1993**, *32*, 21.
(25) Sawicka, A.; Skurski, P.; Hudgins, R.; Simons, J. *J. Phys. Chem. B* **2003**, *107*, 13505.
(26) Hodgkins, P.; Fairman, M.; ONeill, P. *Radiat. Res.* **1996**, *145*, 24.
(27) Sunderland, C. J.; Steiert, M.; Talmadge, J. E.; Derfus, A. M.; Barry, S. E. *Drug Dev. Res.* **2006**, *67*, 70.
(28) Rosi, N.; Giljohann, D.; Thaxton, C.; Lytton-Jean, A.; Han, M.; Mirkin, C. *Science* **2006**, *312*, 1027.
(29) Tkachenko, A.; Xie, H.; Coleman, D.; Glomm, W.; Ryan, J.; Anderson, M.; Franzen, S.; Feldheim, D. *J. Am. Chem. Soc.* **2003**, *125*, 4700.
(30) Klein, O.; Nishina, Y. *Z. Phys.* **1929**, *52*, 853.
(31) Joy, D.; Luo, S. *Scanning* **1989**, *11*, 176.
(32) Foos, E. E.; Snow, A. W.; Twigg, M. E. *J. Cluster Sci.* **2002**, *13*, 543.
(33) Wang, G. L.; Zhang, J.; Murray, R. W. *Anal. Chem.* **2002**, *74*, 4320.
(34) Method of Monte Carlo simulation: A detailed description of the Monte Carlo method is given in the Supporting Information. In brief, each of the following steps was modeled. First, X-rays from a 100-kVp tungsten target were absorbed by water and gold nanoparticles to produce electrons. The photoelectrons and Compton electrons (via Klein-Nishina cross sections) generated in water and photoelectrons and Auger electrons generated in gold were considered.[30] These electrons then interacted with gold to generate secondary electrons, modeled by a modified Bethe formula.[31] All of these electrons were attenuated by water, which produced hydroxyl radicals. The energy deposition density of electrons was estimated for nanoparticles. The density should be proportional to the distribution of the radicals before the diffusion of the radicals was considered.
(35) Gold nanoparticles, their conjugation to scDNA, and radiation experiments: The detailed description is given in the Supporting Information. In brief, triethylene glycol (TEG) coated nanoparticles synthesized using the method of Foos et al. were coated with a few to a few tens of an ethidium-based thiol ligand from Wang et al.[32,33] Nanoparticle−scDNA conjugates were then prepared by diluting stock DNA solution to 100 ng in 5 μL in water and combining this with 10 μL of appropriate concentrations of nanoparticle in water and an additional 5 μL of Tris base in water. The control samples contained the same amount of scDNA and Tris base, but 10 μL of water was added in place of the nanoparticle solution. When samples required radiation, the total 20 μL volume was irradiated with a 100 kVp tungsten radiation unit (HP Faxitron, 43855A) and analyzed using gel electrophoresis. The gel results were analyzed using Chemidoc XRS software from Bio-Rad.